THE ASTROPHYSICAL JOURNAL, 303:451–464, 1986 April 1

GROUND-BASED AND *IRAS* OBSERVATIONS OF COMPACT PLANETARY NEBULAE[1]

SUN KWOK,[2] BRUCE J. HRIVNAK,[2] AND E. F. MILONE[2]
Department of Physics, The University of Calgary
Received 1985 August 19; accepted 1985 September 20

ABSTRACT

A group of compact planetary nebulae suspected of being young objects from their radio properties were observed in the infrared using the Canada-France-Hawaii Telescope. Combining our results with the data from the *IRAS* satellite, we find that most have far-infrared excesses with color temperatures of ~ 200 K. The free-free emission components are clearly distinguished from the dust components and are consistent with the levels of continuum emission expected from radio measurements. For the first time, the total bolometric fluxes of the nebulae have been measured, and the results suggest that the dust in these compact nebulae are heated by direct starlight rather than by nebular Lyman-α photons. We also find a clear correlation between the dust optical depth and the radio surface brightness temperature, suggesting that the dust optical depth is monotonically decreasing with age and the dust component is dispersing into the interstellar medium. The similarity of the infrared spectra of these young nebulae with those of late asymptotic giant branch stars supports the 1980 suggestion of Kwok that the far-infrared dust emission of planetary nebulae originates from the remnants of the circumstellar envelopes of their red giant progenitors.

Subject headings: infrared: sources — nebulae: planetary — stars: circumstellar shells

I. INTRODUCTION

Before the advent of infrared technology in the 1960s the infrared spectra of planetary nebulae were expected to be dominated by atomic line emissions. The discovery of strong infrared continuum emission from planetary nebulae (Gillett, Low, and Stein 1967) therefore came as a surprise to many astronomers. It was soon realized that dust grains are responsible for the infrared emissions from planetary nebulae and many of the observed spectral features are grain features. The common occurrence of dust in planetary nebulae was demonstrated by Cohen and Barlow's (1974) survey of >100 nebulae using the 1.5 m UM-UCSD telescope at Mount Lemmon. Although a number of the grain features (e.g., at 3.3, 6.2, 7.7, 8.6, and 11.3 μm) remain unidentified, some planetary nebulae do show familiar grain features of silicate and silicon carbide grains (Aitken and Roche 1982), which are common in the circumstellar envelopes of asymptotic giant branch (AGB) stars. Since planetary nebulae are generally believed to descend from AGB stars, it has been suggested that the dust emission from the remnant circumstellar envelopes of their AGB progenitors should still be observable in young planetary nebulae (Kwok 1980, 1982). It is therefore interesting to attempt to trace the evolution from AGB to planetary nebulae by observing the dust spectrum of the circumstellar envelope as it gradually disperses into the interstellar medium. Such observations would allow us to fill in the evolutionary gap now existing between the AGB and planetary nebulae phases. In this paper we present infrared observations of a number of planetary nebulae which are inferred to be young by their radio properties (Kwok 1985) and discuss the implications of the infrared observations on the evolutionary status of these objects.

[1] Publication of the Rothney Astrophysical Observatory, No. 35.
[2] Visiting Astronomer at the Canada-France-Hawaii Telescope, operated by the National Research Council of Canada, the Center National de Recherche Scientifique of France, and the University of Hawaii.

II. GROUND-BASED OBSERVATIONS

Our observations were all made with the 3.6 m Canada-France-Hawaii Telescope (CFHT) on Mauna Kea. The telescope was in the f/35 infrared configuration, as described by Maillard and Dyck (1982). Two detector units were used, an InSb photometer for bandpasses in the wavelength interval 1.25–3.8 μm, and a Ge bolometer for the wavelength interval 7.8–25 μm. The central wavelength and full width half-maximum (FWHM) values of the filters used with each detector are listed in Table 1. Apertures of 8″ and 4″.7 were used for the InSb and Ge bolometers respectively, with a throw of 16″ in declination. Observations were primarily obtained during 1984 May 10–14 with the exception of the bolometer measurements of IC 5117, K3-62, and Me 2-2 which were made during 1984 August 12–16 with an aperture of 10″.7. Infrared standard stars were observed each night and were used to reduce the observations to standard magnitudes. The conversion factors to flux for a 0.00 mag star are also given in Table 1 and are taken primarily from Hanner *et al.* (1984) except L', 7.8 μm, and Q. The conversions to flux at L' and 7.8 μm were accomplished by interpolation on a plot of log F_λ versus log λ of the absolute flux calibration of Hanner *et al.* (1984), while that at Q is discussed separately below.

The observations made with the InSb photometer were first corrected for extinction, with linear extinction coefficients obtained from the observations of four infrared standard stars each night. The JHK magnitudes were then transformed to the CIT standard system, or more precisely, to a subset of infrared standard stars, from the list of Elias *et al.* (1982). These procedures necessitated nightly zero-point corrections and then mean color terms from the two nights were included in the transformations. For the L' bandpass, published standards were not available at the time of the observations. Such a list of standard star magnitudes has recently been published by Sinton and Tittemore (1984). Unfortunately we observed none of these standard stars. However, we are able to make an

TABLE 1

INFRARED FILTER CHARACTERISTICS

Band	Central Wavelength (μm)	FWHM (μm)	F_ν for 0.0 Mag (Jy)
InSb Photometer			
J	1.25	0.30	1510
H	1.65	0.29	980
K	2.22	0.43	620
L'	3.80	0.60	230
Ge Bolometer			
... .	7.8	0.7	61
... .	8.7	1.2	49
... .	9.8	1.2	39
... .	10.3	1.0	35
N	10.5	5.1	34
... .	11.6	1.3	28
... .	12.5	1.2	24
Q	20	9	9.8
... .	25	10	6.5

approximate transformation of the measurements of our standard stars to their L' systems by using their published relationship between the L' magnitudes and the L magnitudes of Elias *et al.* (1982). We note that this involves an extrapolation for our red program objects beyond the color regime investigated by Sinton and Tittemore and introduces some additional uncertainty into our standardized L' magnitudes.

The final standard magnitude values of the program objects are listed in Table 2. The accuracy of the standard star observations on the *CIT* standard system is ± 0.03 mag in magnitudes and ± 0.01 mag in color. Since our signal-to-noise ratio is very high in all filters except L', we believe the accuracy of our observations on the standard system to be ± 0.04 mag in JHK and ± 0.08 mag in L'. In several cases the objects were not detected at particular bandpasses, and upper limits were set at 3 σ, where σ is the standard deviation among the measurements in an observation.

The observations made with the helium-cooled Ge bolometer were first corrected for extinction, with mean extinction coefficients for each filter derived from the nightly values. The values for each night were not significantly different from each other. The object α Lyr was the primary standard used for both extinction and to transform the observations to a standard system in the wavelength interval 7.8–12.5 μm. Since it is a weak source at 20 and 25 μm, we observed additional infrared standards in these bandpasses once or twice each night for calibration purposes. The additional standards were BS 0337 (β And), BS 4069 (μ UMa), and BS 8316 (μ Cep). It should be noted that the latter two of these standards have recently been suggested to be somewhat variable (Sinton and Tittemore 1984). This suggested variability is incorporated into the error estimates of our final results given below.

The fluxes were transformed to standard magnitudes using nightly zeropoint values derived from α Lyr and the other standard stars. In the wavelength interval 7.8–12.5 μm, α Lyr was assumed to have a magnitude of 0.00 in each bandpass. At 20 μm the data were transformed to a standard system based upon the additional standards listed above, using standard magnitudes from Tokunaga (1984) and Hanner *et al.* (1984). At 25 μm, standard magnitudes have not been published for any of these standards. Therefore, we calculated the absolute flux of the three additional standards by a linear extrapolation of their spectra on a plot of log F_λ versus log λ, using the absolute flux calibration of Hanner *et al.* (1984). We then converted this to the magnitude scale through a similar extrapolation of the absolute flux density for a 0.00 mag star.

The standardized magnitudes in the bolometer passbands are listed in Table 2 along with the final InSb magnitudes. Based upon the signal-to-noise ratio of our observations and the uncertainties in standardization, we believe a conservative estimate of the accuracy of the bolometer data to be ± 0.15 mag at the shorter wavelengths, and ± 0.20 mag and ± 0.30 mag at 20 μm and 25 μm, respectively, except where noted otherwise. In several cases where the objects were not detected, we set upper limits at 3 σ.

III. RESULTS

Among the 15 planetary nebulae observed with the bolometer at the CFHT, eight were detected at 10.5 μm and six at 20 μm. Since the *IRAS Point Source Catalog* became available in

TABLE 2

OBSERVATIONAL DATA

PK Number	Name	J	H	K	L'	[7.8]	[8.7]	[9.8]	[10.3]	N	[11.6]	[12.5]	Q	[25]
010+18°1	K2-8	...	...	...	...	...	...	...	...	>6.1	...	...	...	...
010+18°2	M2-9	...	...	...	...	0.69	0.43	0.20	0.12	−1.1	−0.52	−0.77	−1.83	−1.8
018+20°1	Na-1	>16.2	...	...	...	...	...	...	...	...	...	...	...	...
027−9°1	IC 4846	12.16	12.44	11.75	10.66	...	...	...	...	>6.5	...	...	...	...
028+5°1	K3-2	13.25	12.89	12.14	10.78	...	...	...	...	6.5[a]	...	...	...	...
042−6°1	NGC 6807	12.37	12.81	12.06	10.72	...	...	...	...	>5.7	...	...	...	...
051+9°1	Hu 2-1	12.17	12.39	11.65	...[b]	...	...	...	...	...	...	...	...	...
071−2°1	M3-35	11.42	11.16	9.97	7.87	3.00	2.99	2.48	2.20	2.32	1.56	1.36	−0.74	−0.8
082°+11°1	NGC 6833	12.26	12.61	11.98	10.65	...	...	...	...	>6.6	...	...	...	...
089−5°1	IC 5117	12.08	11.82	10.58	...	2.39	2.34	1.97	1.66	1.69	0.93	0.89	−1.14	−1.9
095+0°1	K3-62	12.42	12.00	10.89	9.22	5.3[a]	4.62	4.77	3.68	3.68	2.76	2.39	0.23	>−1.2
100−8°1	Me 2-2	...	...	...	...	>4.8	5.26	4.22	4.16	4.08	3.21	2.71	0.82	>−2.1
212+4°1	M1-9	12.60	12.96	12.12	10.97	>3.6	...	>4.5	...	6.2[a]	...	...	...	...
342+27°1	Me2-1	...	...	...	...	...	...	...	...	>5.8	...	...	...	...
356+4°1	M2-11	13.35	13.58	12.72	11.25	...	...	...	...	>6.4	...	...	...	...
356+4°1	M3-38	11.96	10.83	10.54	...[b]	...	...	...	...	>6.4	...	...	...	...
358+5°2	M3-40	13.10	12.42	11.81	...[b]	>4.6	>5.6	>5.4	>4.4	5.28	...	...	1.46	>0.2

[a] Error estimate of ± 0.5 mag.

[b] Sky saturated.

TABLE 3

IRAS OBSERVATIONS

Nebula	Color Temperature Used for Correction (K)			Correction Factors				Corrected Flux Density (Jy)			
	T_{12}	T_{23}	T_{34}	12 μm	25 μm	60 μm	100 μm	12 μm	25 μm	60 μm	100 μm
K2-8	...	...	...	...	...	...	...	...	...	...	...
M2-9	21.4	130	116	0.839	0.986	1.068	1.045	60.3	111.7	115.3	71.9
K3-2	128	155	...	0.907	0.932	1.111	...	0.42	6.0	4.0	<7.2
Na-1	...	103	...	...	0.850	1.025	...	<0.25	1.5	2.7	<1.6
IC 4846	...	156	...	...	0.961	1.112	...	<0.34	4.1	2.8	<1.7
NGC 6807	141	401	52	0.867	1.076	1.076	0.993	0.61	4.6	1.3	2.1
Hu 2-1	158	190	...	0.838	0.995	1.149	...	2.49	12.3	6.0	<4.3
M3-35	180	426	...	0.825	1.117	1.245	...	7.68	21.0	5.2	<35.0
IC 5117	174	203	14593	0.827	1.020	1.240	1.090	13.66	46.1	19.4	7.8
K3-62	155	212	...	0.842	1.010	1.168	...	2.44	12.9	5.4	<32.1
Me 2-2	185	312	...	0.824	1.091	1.214	...	1.49	3.8	1.1	<1.3
M1-9	163	183	...	0.834	0.993	1.144	...	0.43	1.9	1.0	<6.3
Me 2-1	...	185	...	...	1.016	1.146	...	<0.25	2.8	1.4	<1.0
M2-11	...	135	...	...	0.920	1.086	...	<1.50	2.0	1.7	<1.1
M3-38	164	119	...	0.833	0.932	1.064	...	1.46	6.7	8.1	<16.2
M3-40	...	133	...	...	0.916	1.083	...	<0.73	6.8	6.1	<10.7

early 1985, we have performed a search through the *Catalog* and found 15 of our 17 program sources to have far-infrared excesses. Since the *IRAS* filters have broad bandpasses (Neugebauer *et al.* 1984), color corrections are necessary to obtain reliable flux values at the centers of the filters. The color temperatures (T_{ij}) were determined between adjacent *IRAS* bands i and j and the correction factors were derived by interpolation using correction factors listed in Table VI.C.6 of the *IRAS Catalog* and *Atlas Explanatory Supplement*. For bands (25 and 60 μm) with two adjacent bands, the two correction factors are averaged before they are applied. The corrected flux densities and color temperatures used for correction are given in Table 3.

The combined CFHT and *IRAS* spectra of our 15 program sources are plotted in Figures 1–15. Sample blackbody curves (normalized with respect to the 60 μm point) are also shown for comparison purposes. In the cases where InSb observations were made, the observed fluxes in the near-infrared are often in excess of the flux levels of the cool dust component. These excesses are probably due to thermal free-free emission from the ionized nebulae. We have plotted expected levels of free-free emission extrapolated to the infrared from the 5 GHz flux,

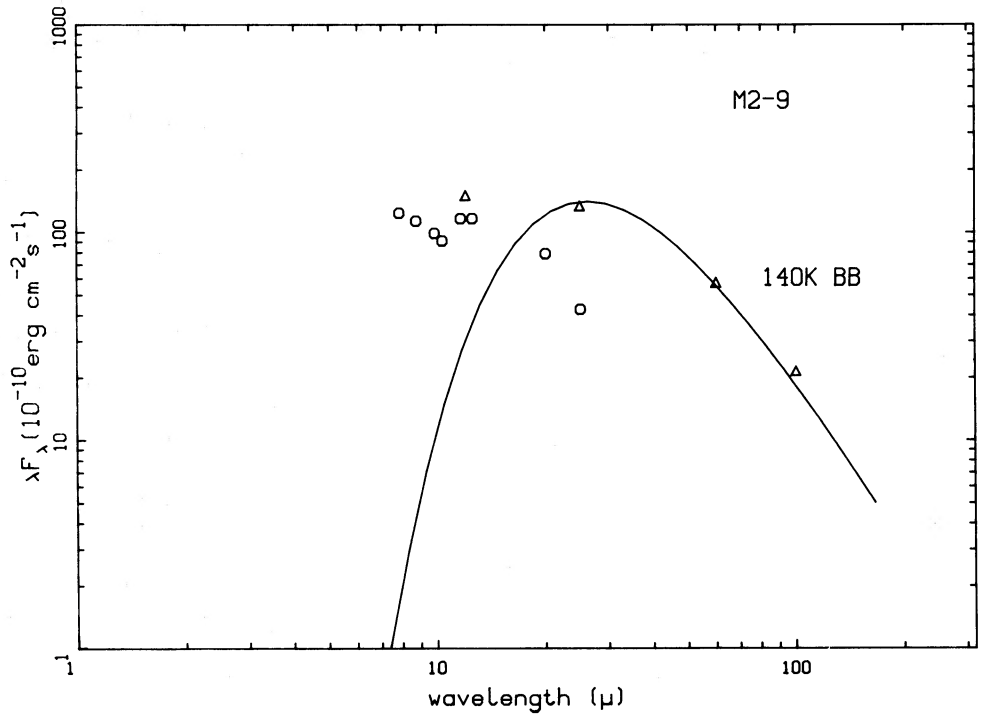

FIG. 1.—Infrared spectra of the compact planetary nebula M2-9. The circles are CFHT measurements, the triangles are *IRAS* measurements, and inverted triangles are upper limits. Blackbody curves are also shown for comparison. The dashed lines show the level of free-free emission extrapolated from 5 GHz radio fluxes.

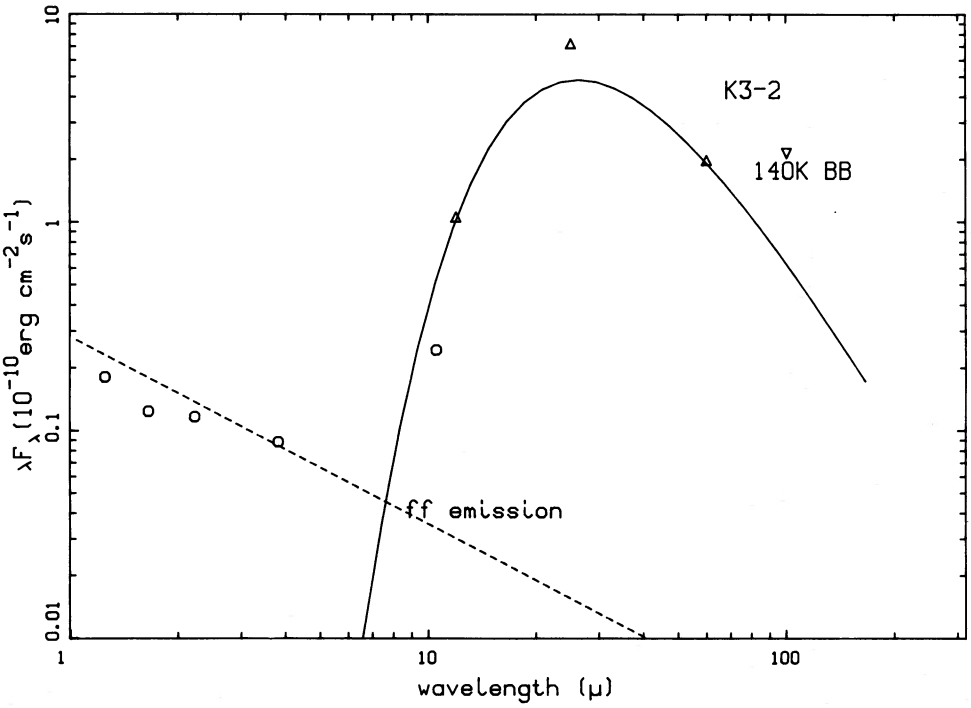

FIG. 2.—K3-2

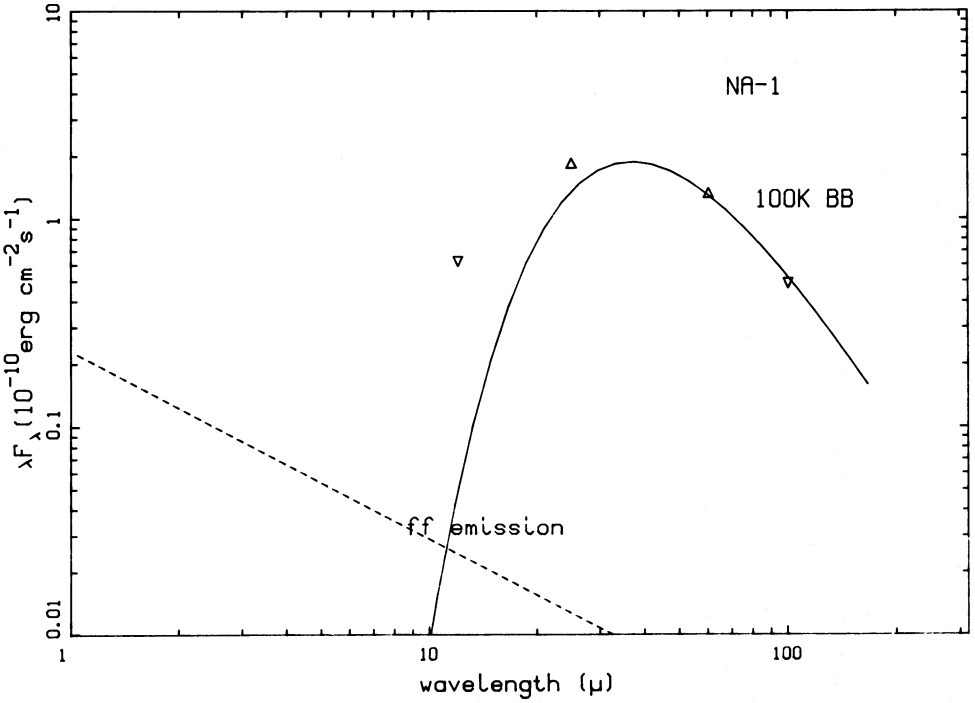

FIG. 3.—Na-1

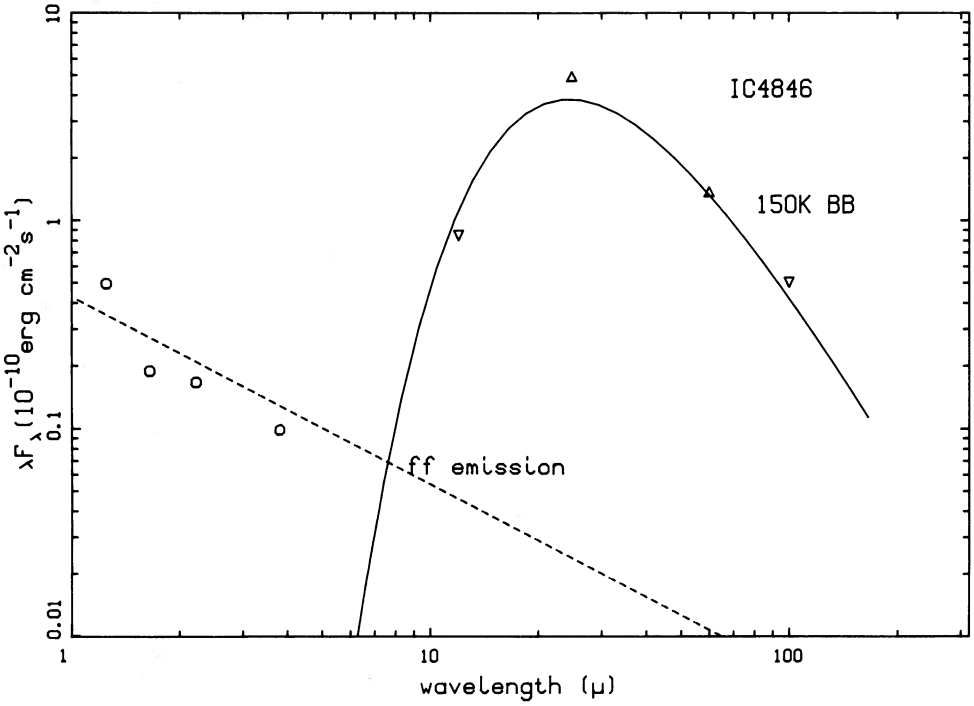

FIG. 4.—IC 4846

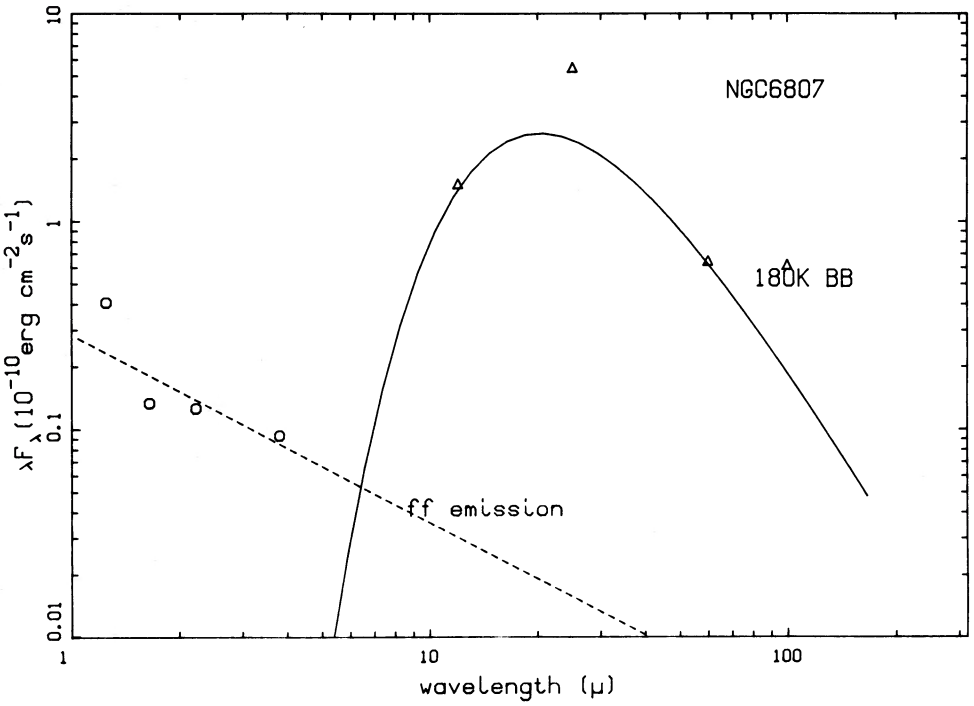

FIG. 5.—NGC 6807

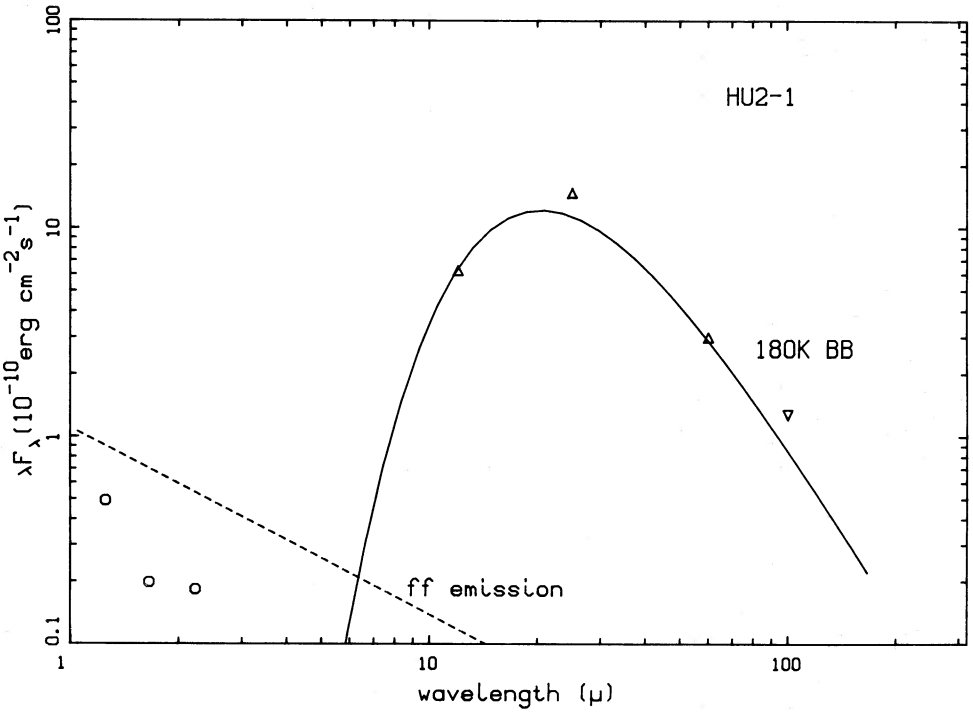

FIG. 6.—Hu 2-1

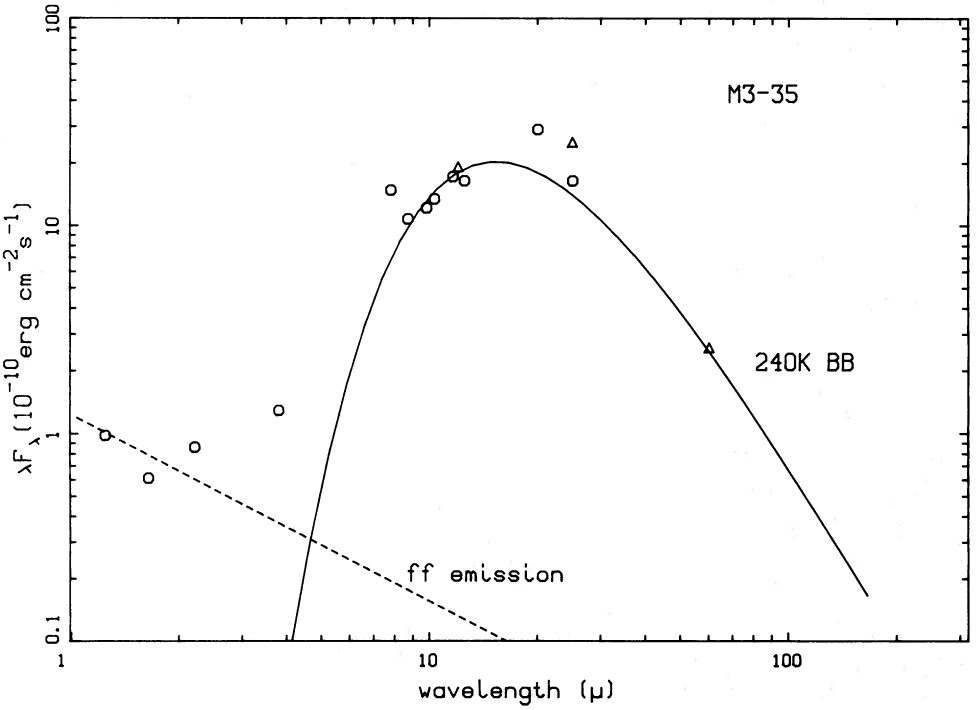

FIG. 7.—M3-35

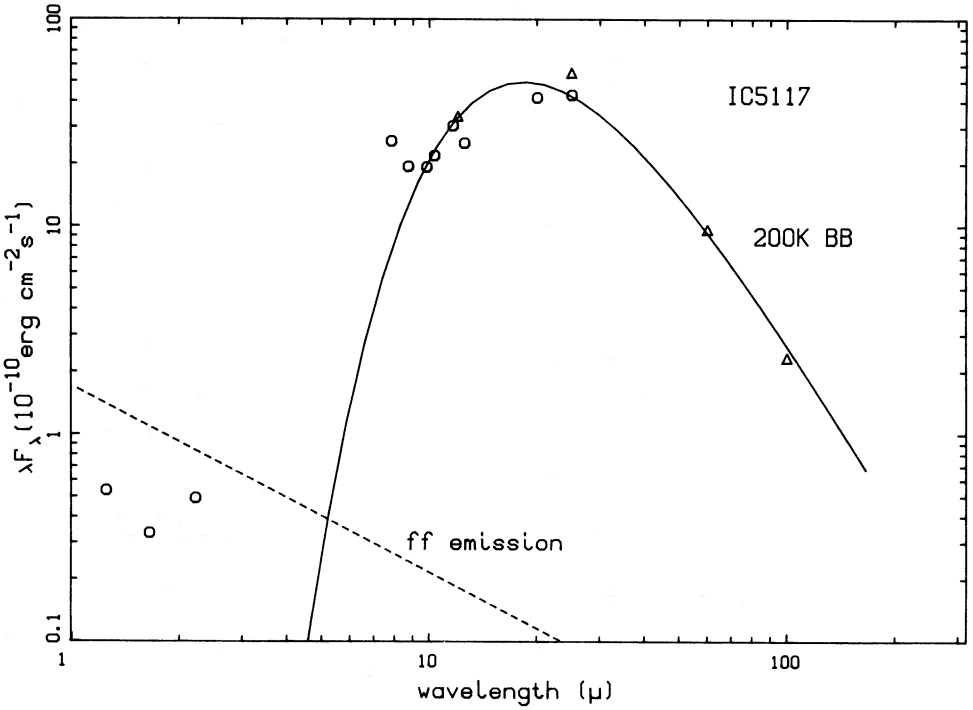

FIG. 8.—IC 5117

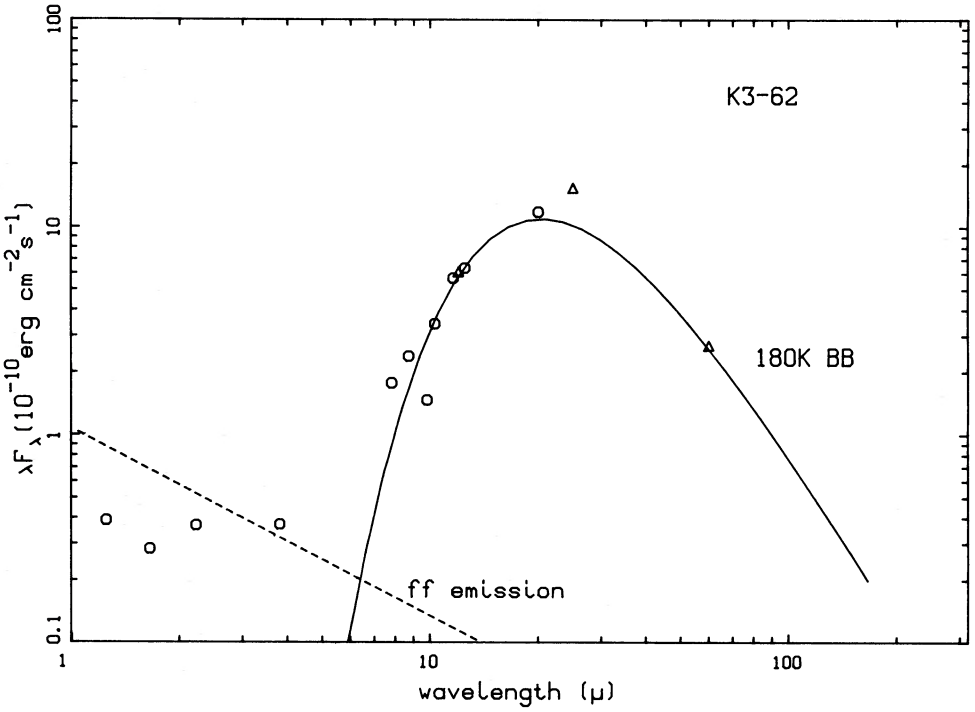

FIG. 9.—K3-62

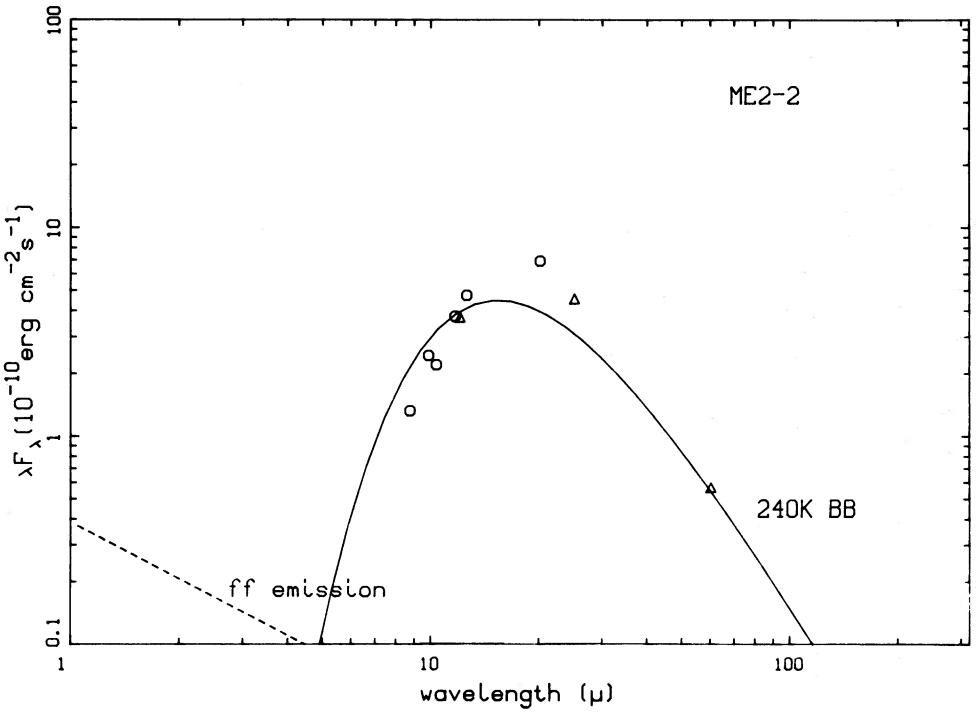

FIG. 10.—Me 2-2

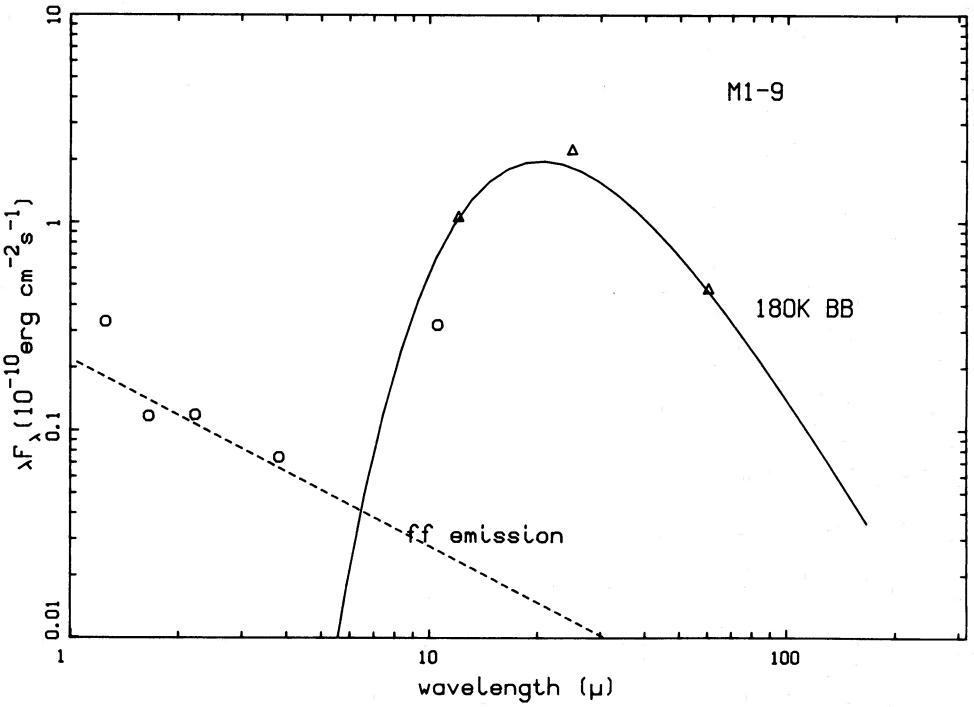

FIG. 11.—M1-9

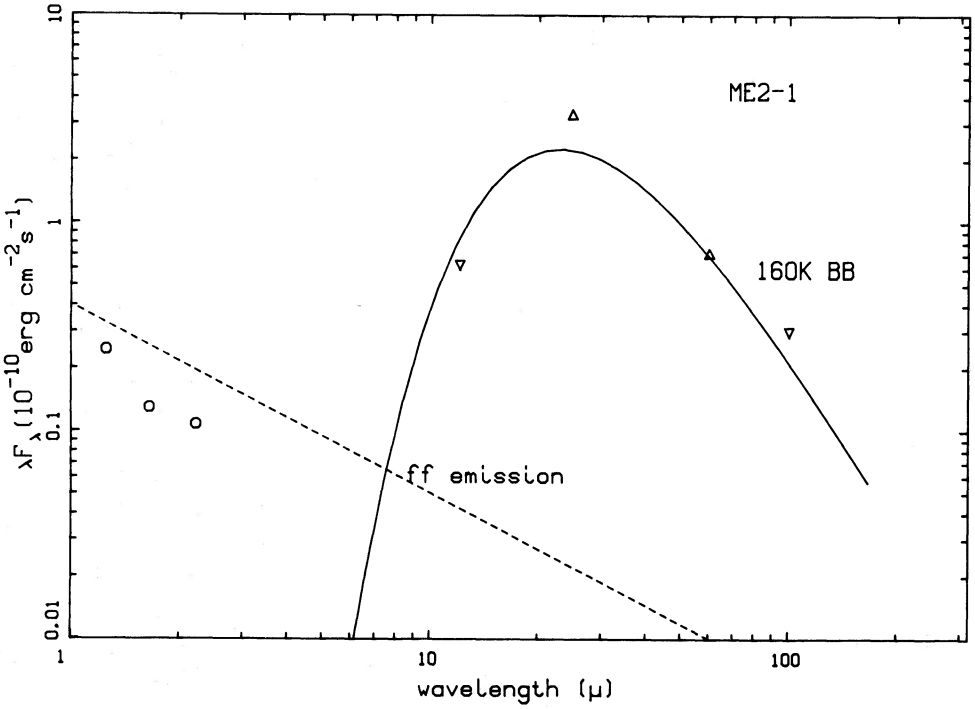

FIG. 12.—Me 2-1

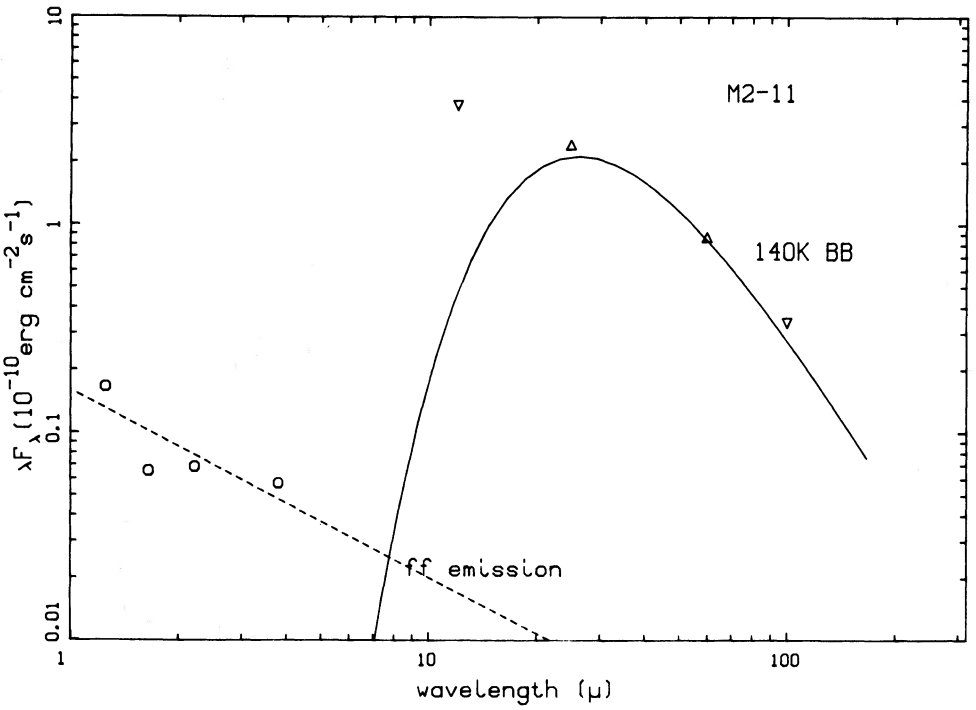

FIG. 13.—M2-11

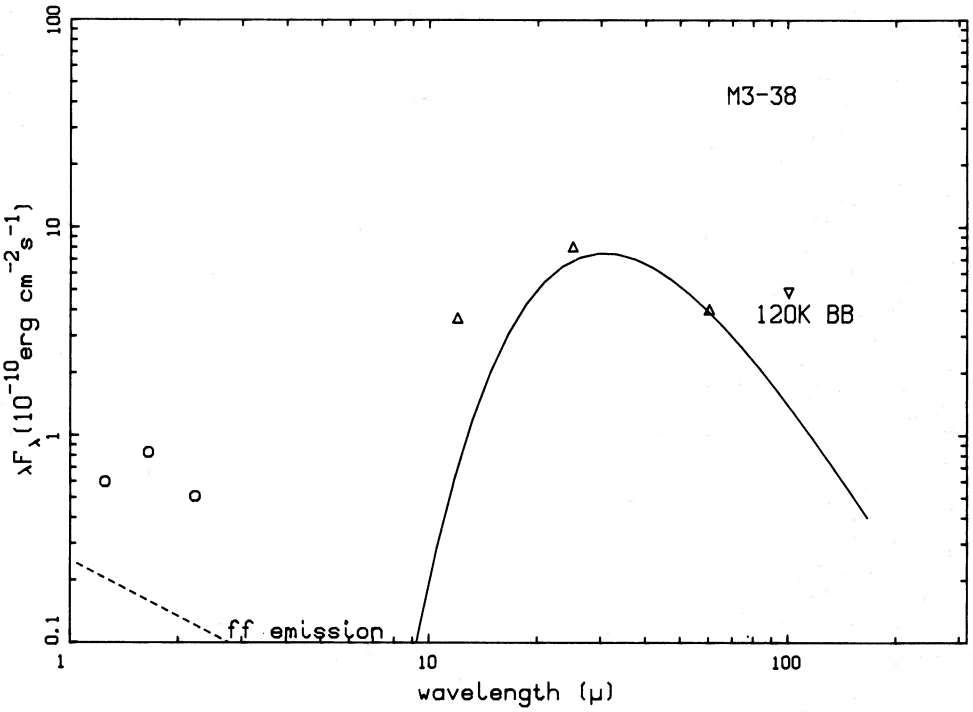

FIG. 14.—M3-38

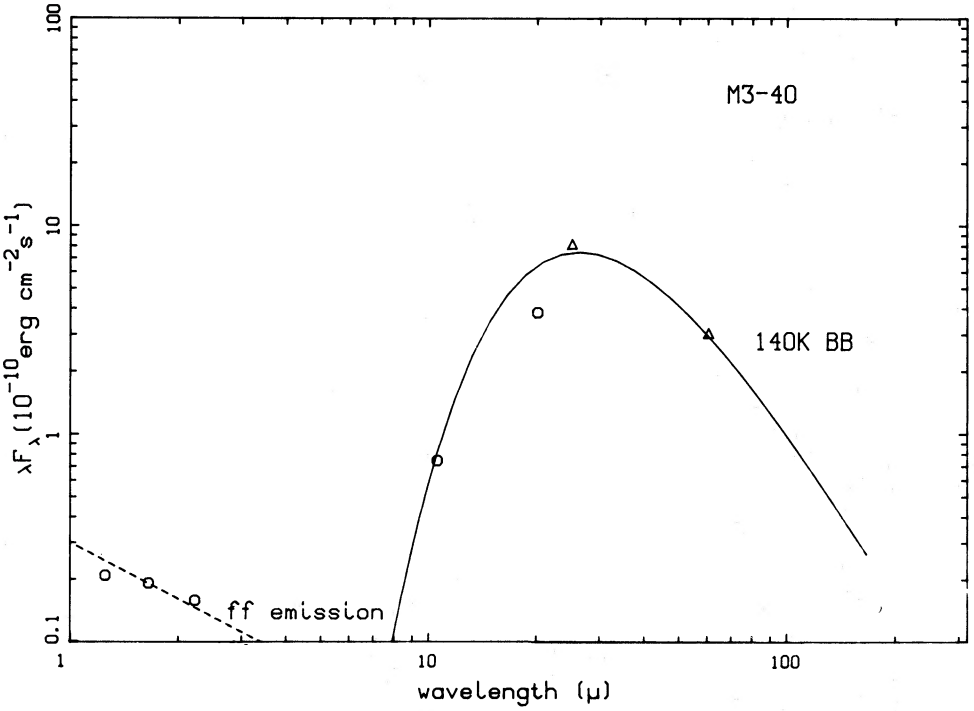

FIG. 15.—M3-40

assuming that $F_\nu \propto \nu^{-0.1}$. The agreement between the InSb measurements and the predicted level of free-free emission is remarkable considering that the extrapolation is made over four decades in frequency. Existing discrepancies are probably due to bound-free emission, the Paschen and Brackett jumps, and contribution from recombination lines.

We can see from Figures 1–15 that most of the energy of these nebulae is emitted in far-infrared wavelengths, and their total observed fluxes can be estimated by integrating over their infrared spectra. This was done by one of the following two methods. For objects that have adequate measurements to cover the complete spectrum, the area under the spectrum was approximated by a series of rectangles. Beyond 40 μm, the area is calculated assuming the Rayleigh-Jeans law:

$$\int_{40\ \mu\mathrm{m}}^{\infty} F_\lambda\, d\lambda = \frac{2ckT}{3}\,\phi^2(40\ \mu\mathrm{m})^{-3}\,, \qquad (1)$$

where

$$\phi^2 = \frac{(\lambda F_\lambda)_{60\ \mu\mathrm{m}}}{\pi(\lambda B_\lambda)_{60\ \mu\mathrm{m}}}\,.$$

The reference wavelength of 60 μm is chosen for the normalization factor ϕ because 60 μm lies on the Rayleigh-Jeans part of the spectrum, and most objects are detected in the *IRAS* 60 μm band. Since most of the energy is emitted between 10 and 20 μm, the Rayleigh-Jeans approximation does not have serious effects on the results. For objects that have only broad-band measurements (e.g., M1-9), the total dust emission is calculated using the blackbody formula

$$F_{\mathrm{IR}} = \phi^2\pi \int_0^{\infty} B_\lambda\, d\lambda = \phi^2\sigma T^4\,, \qquad (2)$$

where σ is the Stefan-Boltzmann constant. The fluxes measured by the InSb detector (which presumably arise from free-free emission) are summed separately. Results of these calculations together with other physical properties of the nebulae are given in Table 4. The accuracy of the derived fluxes varies from object to object and is about 10% in the best cases.

The nebula M2-9 is an anomaly in our sample. It is a bipolar nebula of angular size 40″ × 10″. Although M2-9 cannot qualify as a compact planetary nebula it has often been suggested to be young. Infrared observations have been made by Cohen and Barlow (1974), Eiroa, Hefele, and Qian (1983), and Aitken and Roche (1982). M2-9 has a broad energy distribution with a color temperature of ~690 K from 2 to 4 μm, and a much lower (~140 K) color temperature in the far-infrared. The total flux given in Table 4 includes contribution from both components. Our CFHT observations only includes the core of M2-9 and do not detect any of the extended emission present. Comparison of our ground-based data with the *IRAS* measurements show that while there is agreement in the near-infrared (12.5 μm band), our 20 and 25 μm measurements are substantially below the 25 μm flux of *IRAS*. This suggests that the cool dust component is much larger in size than that of the core.

IV. THE DUST HEATING MECHANISM

The possibility that dust in planetary nebulae can be heated by Lyman-α (Lyα) radiation was first suggested by Krishna Swamy and O'Dell (1968). The mechanism responsible for heating of the dust has been extensively discussed by Cohen and Barlow (1974, 1980) and Grasdalen (1979). This question could not be satisfactorily resolved in the past because a significant amount of radiation from planetary nebulae is emitted at wavelengths longward of those accessible from the ground, and thus the total infrared flux was never very accurately deter-

TABLE 4

PHYSICAL PARAMETERS OF THE OBSERVED NEBULAE

Nebula	R.A. (1950)	Decl. (1950)	Angular Diameter (arcsec)	$F_{5\ \mathrm{GHz}}$ (mJy)	$F_{\mathrm{IR(dust)}}$ (10^{-10} ergs cm^{-2} s^{-1})	$F_{1-6\ \mu\mathrm{m}}$ (10^{-10} ergs cm^{-2} s^{-1})
K2-8	17^{h}02^{m}45^s.3	−10°01′40″ [a]	...	<10 [b]	...	...
M2-9 [b]	17 02 52.60	−10 04 31.0	40 × 10	25	270	...
Na-1 [c]	17 10 14.43	−03 12 29.0	5	23	2.6	...
IC 4846 [d]	19 13 44.32	−09 07 59.2	2.3	42.9	5.9	0.39
K3-2 [d]	18 22 24.99	−01 32 36.8	2.5	28.2	7.5	0.23
NGC 6807 [e]	19 32 05.79	05 34 25.5	0.9	28.4	3.6	0.32
Hu 2-1 [d]	18 47 38.60	20 47 08.0	1.5	110	17	0.32
M3-35 [d]	20 19 04.71	32 19 49.1	1.5	124	35	1.9
NGC 6833 [e]	19 48 20.85	48 50 01.1	0.7	20.3	...	0.35
IC 5117 [d]	21 30 36.76	44 22 28.5	1.6	172	64	0.53
K3-62 [d]	21 30 09.02	52 20 34.0	2.5	107	16	0.69
Me 2-2 [e]	22 29 37.77	47 32 37.1	1.2	38.4	6.7	...
M1-9 [d]	07 02 42.29	02 51 35.5	2.0	22	2.7	0.27
Me 2-1 [e]	15 19 23.16	−23 26 48.4	5	40.3	3.1	...
M2-11	17 17 23.1	−28 57 40 [f]	<5 [g]	16 [g]	2.9	0.16
M3-38 [c]	17 17 54.20	−29 00 03.4	2	25	10	0.70
M3-40	17 19 20.8	−27 05 45 [f]	<5 [g]	30 [g]	10	0.21

[a] Blackwell and Purton 1981.
[b] Kwok *et al.* 1985.
[c] Kwok, Purton, and Keenan 1981.
[d] Kwok 1985.
[e] Aaquist and Kwok 1986.
[f] Milne 1976.
[g] Milne 1979.

mined. Since most of our program sources have well-defined infrared spectra and high-quality radio observations have been obtained at the Very Large Array, we are now in a much better position to address the problem of the heating mechanism.

The 5 GHz radio fluxes of the nebulae are given in Table 4. With the possible exception of M 3-35, IC 5117, and Me 2-2, the nebulae are all optically thin at 5 GHz. Pottasch (1984) has derived a relationship between the 5 GHz flux density and the total infrared flux assuming all Lyα photons produced by recombination heat the dust:

$$F_{\rm IR} = 6.32 \times 10^{-12} F_{5\ \rm GHz}(\rm mJy)\ \rm ergs\ cm^{-2}\ s^{-1}\ . \quad (3)$$

For nebulae of high density ($n_e > 10^4$ cm^{-3}), this relationship becomes:

$$F_{\rm IR} = 9.38 \times 10^{-12} F_{5\ \rm GHz}(\rm mJy)\ \rm ergs\ cm^{-2}\ s^{-1}\ . \quad (4)$$

In Figure 16, we have plotted the 5 GHz flux against the total infrared flux $F_{\rm IR}$ of the cool-dust component. It is apparent that most of the sources lie to the right of the theoretical curves, and Lyα radiation does not seem to have adequate power to be entirely responsible for dust heating.

This result is not entirely surprising. As noted by Pottasch *et al.* (1984), young planetary nebulae with low-temperature central stars emit a large fraction of their radiative energy longward of the Lyman continuum; thus, the effect of Lyα heating is reduced. Heating by direct starlight is the most plausible cause of dust heating.

An alternative source of heating is the dissipation of the mechanical flux from the star. Present estimates of the mass loss rates from the central stars of planetary nebulae by Cerruti-Sola and Perinotto (1985) suggest that the stellar wind carries only a few percent of the radiative luminosity and therefore should not have a major effect on the observed infrared luminosity.

We note from Figure 16 that M2-9 seems to have far more flux in the infrared by dust emission than in the radio by free-free emission. This could result from M2-9 being ionization-bounded with much of the infrared emission originating from the neutral gas outside of the ionized nebula. The possibility that bipolar nebulae are ionization bounded has been discussed by Calvet and Peimbert (1983) and Kwok *et al.* (1985) for M2-9 and by Kwok and Bignell (1984) for GL 618.

V. ORIGIN OF THE FAR-INFRARED EXCESS

It is clear from Figures 1–15 that these objects, with the exception of M2-9, are very similar in their infrared properties. They all have blackbody-like dust spectra with color temperatures of ~200 K. The observed color temperatures of these nebulae are also significantly higher than those observed for extended nebulae (Pottasch *et al.* 1984). Since many of the nebulae in our sample have high radio surface brightness (Kwok 1985) and are therefore likely to be young planetary nebulae, their high dust temperatures are consistent with the suggestion of Pottasch *et al.* (1984) that smaller and younger nebulae have hotter dust.

For an optically thin sphere of angular radius θ and temperature T, the observed flux is given by

$$F_\lambda = \pi B_\lambda(T)\theta^2(\tfrac{2}{3}\tau_\lambda)\ . \quad (5)$$

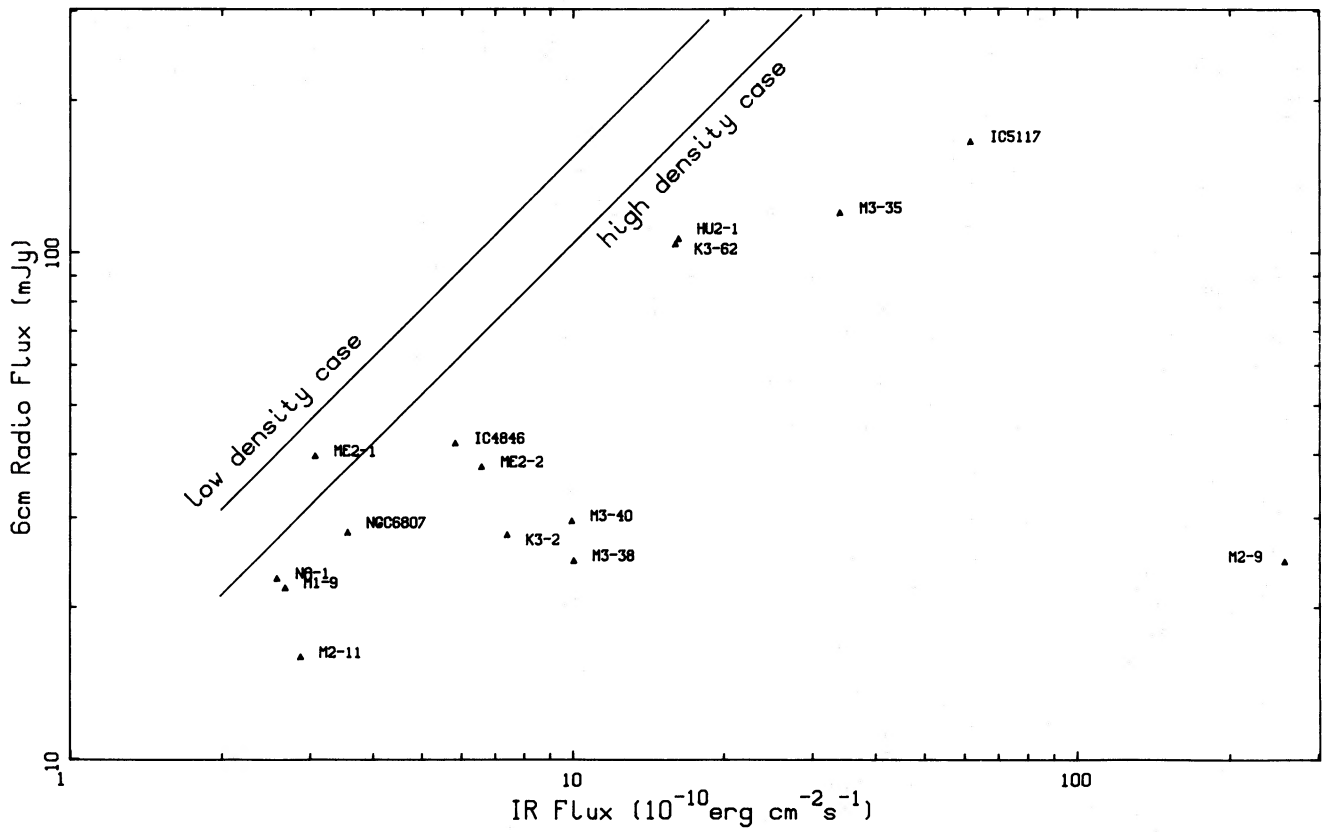

FIG. 16.—Total infrared flux of each nebula is plotted against the 5 GHz radio flux. The two lines are the relations expected if the dust is heated by Lyman-α photons completely trapped in the nebula (cf. Pottasch 1984).

TABLE 5

DERIVED OPTICAL DEPTHS AND BRIGHTNESS TEMPERATURES OF PLANETARY NEBULAE

Nebula	τ (60 μm)	T_b (5 GHz) (K)	Nebula	τ (60 μm)	T_b (5 GHz) (K)
Na-1	4.8(−4)	6.5(1)	NGC 4361	6.6(−6)	3.7(0)
IC 4846	9.2(−4)	5.7(2)	He 2-131	2.2(−3)	5.1(2)
K3-2	1.1(−3)	3.2(2)	NGC 6072	3.0(−4)	2.2(0)
NGC 6807	2.0(−3)	2.5(3)	NGC 6153	9.4(−4)	6.0(1)
Hu 2-1	3.3(−3)	3.5(3)	NGC 6210	3.2(−4)	7.2(1)
M3-35	1.8(−3)	3.9(3)	NGC 6302	2.1(−3)	1.2(2)
IC 5117	7.8(−3)	4.8(3)	NGC 6543	1.6(−3)	2.3(2)
K3-62	1.1(−3)	1.2(3)	NGC 6572	6.7(−4)	4.3(2)
Me 2-2	5.8(−3)	1.9(3)	NGC 6751	1.4(−4)	9.7(0)
M1-9	3.1(−4)	3.9(2)	NGC 6781	2.8(−4)	2.2(0)
Me 2-1	8.6(−5)	1.1(2)	BD +303639	1.0(−2)	1.6(3)
M3-38	5.7(−3)	4.4(2)	NGC 6818	1.7(−4)	6.1(1)
			NGC 6826	2.4(−4)	4.3(1)
NGC 246	1.6(−5)	3.1(−1)	NGC 6884	1.2(−3)	3.9(2)
NGC 1501	4.0(−5)	5.0(0)	NGC 6886	6.1(−4)	1.4(2)
IC 418	6.5(−4)	4.9(2)	NGC 6891	2.6(−4)	4.6(1)
NGC 2346	1.5(−4)	2.0(0)	IC 4997	5.5(−3)	3.5(3)
NGC 2371/2	1.9(−5)	2.2(0)	NGC 6905	1.6(−5)	1.7(0)
NGC 2438	1.0(−4)	1.3(0)	NGC 7008	4.0(−5)	2.4(0)
NGC 2440	1.5(−4)	2.7(1)	NGC 7009	5.0(−4)	7.4(1)
NGC 2818	4.7(−5)	9.1(−1)	NGC 7026	1.8(−3)	1.5(2)
NGC 2867	1.9(−4)	7.5(1)	Hu 1-2	1.6(−4)	1.6(2)
NGC 3242	1.2(−4)	3.6(1)	NGC 7662	3.9(−4)	1.9(2)

Using the color temperatures in Figures 1–15 and the observed *IRAS* flux at 60 μm, we have

$$\tau_{60\,\mu\mathrm{m}} = 1.5(\phi/\theta)^2 \,. \tag{6}$$

Since for most of the nebulae θ's are known from VLA measurements, $\tau_{60\,\mu\mathrm{m}}$ can be derived from equation (6), and the results are given in Table 5. If the 60 μm dust emission originates from a volume significantly larger than the ionized nebula, the values of τ would be smaller.

For comparison optical depths at 60 μm are also calculated for more extended nebulae from data in Tables 1 and 2 of Pottasch *et al.* (1984). We note that the optical depths in our sample of compact nebulae are generally higher. Since θ is not an absolute measurement of age (nebulae can be at different distances), a better indicator for age is needed. One such parameter is the radio surface brightness temperature T_b defined by

$$T_b = \frac{\lambda^2}{2\pi k}\frac{S}{\theta^2}\,, \tag{7}$$

where k is the Boltzmann constant and S is the 5 GHz radio flux density. Figure 17 is a plot of T_b versus $\tau_{60\,\mu\mathrm{m}}$, and a proportional relationship is clearly evident. This suggests that as the ionized gas expands with time, the dust envelope is also expanding and dispersing into the interstellar medium.

If the dust component responsible for the far-infrared emission from planetary nebulae is indeed due to the remnant of the AGB circumstellar envelope as suggested by Kwok (1980), then we must seek an explanation to the apparent monotonically decreasing color temperature from >1000 K for Miras, to 300–600 K for OH/IR stars, to 200 K for young planetary nebulae, and to <100 K for evolved planetary nebulae. It is widely accepted now that the infrared excesses of late-type stars are the results of mass loss (Gehrz and Woolf 1971) and that the decreasing color temperature is the consequence of increasing mass loss rate and optical depth (Merrill 1977). Since Figure 17 suggests that the optical depth of planetary nebulae is in fact decreasing, rather than increasing with time, there must be a point in the evolution of a star that this reversal in τ occurs. The most reasonable hypothesis is that at some point the mass loss stops and the dust envelope detaches from the star and expands. The subsequent decrease in color temperature is the result of geometric dilution in the radiative flux of the central star, which is responsible for heating the dust as discussed in § IV. The detachment of the dust envelope is also found to be a plausible explanation for the *IRAS* colors of some nonvariable OH/IR stars (Bedijn 1985).

VI. CONCLUSIONS

The results of this paper show that far-infrared observations of planetary nebulae provide valuable clues to the early stages of planetary nebulae evolution. Young planetary nebulae are apparently surrounded by the remnant dust envelopes of their AGB progenitors, and such dust envelopes are heated directly by radiation from the central stars. There is also evidence that the dust envelopes have detached from the central stars and are now expanding into the interstellar medium. While the dust optical depth of the circumstellar envelope increases as a star ascends the AGB, the dust optical depth decreases with age in the planetary nebula phase. More observations of young planetary nebulae and evolved AGB stars will allow us to precisely determine the point of envelope detachment and better understand the transition from red giant to planetary nebula.

We acknowledge with gratitude the help provided by Drs. R. McLaren and J. P. Maillard at the CFHT. We also thank R. T. Boreiko for assistance in the August observing run. University of Calgary undergraduates P. Langill and C. T. Haglund assisted in the data analysis. The *IRAS Point Source Catalog* is provided on magnetic tape in machine-readable form by the World Data Center in Greenbelt, Maryland. This work is supported by a grant to S. K. from the Natural Sciences and Engineering Research Council of Canada.

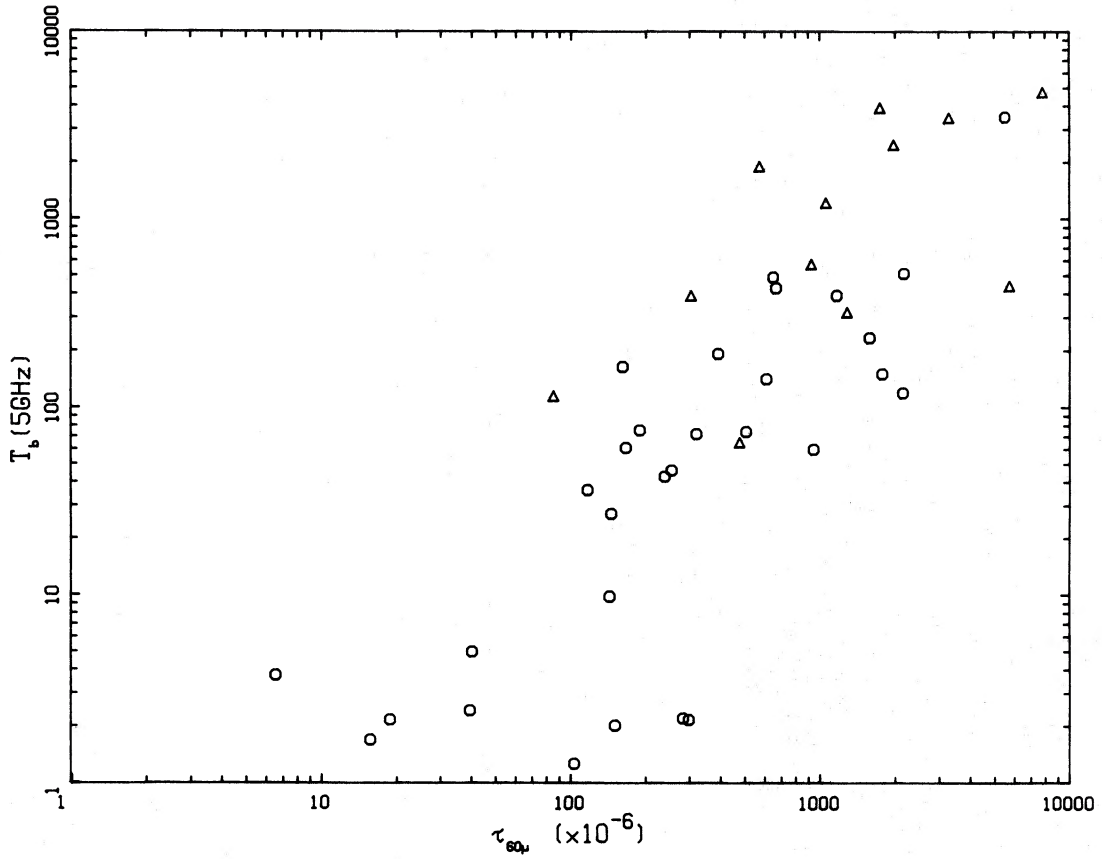

FIG. 17.—Radio surface brightness temperature of planetary nebulae plotted against the derived 60 μm optical depth. Circles are objects in Pottasch *et al.* (1984), and triangles are objects in this paper.

REFERENCES

Aaquist, O., and Kwok, S. 1986, in preparation.
Aitken, D. K., and Roche, P. F. 1982, *M.N.R.A.S.*, **200**, 217.
Bedijn, P. J. 1985, paper presented at the First *IRAS* Symposium, June 10–14, Noordwijk.
Blackwell, J. R., and Purton, C. R. 1981, *Astr. Ap. Suppl.*, **46**, 181.
Calvet, N., and Peimbert, M. 1983, *Rev. Mexicana Astr. Ap.*, Vol. **5**, No. 4, p. 319.
Cerruti-Sola, M., and Perinotto, M. 1985, *Ap. J.*, **291**, 237.
Cohen, M., and Barlow, M. J. 1974, *Ap. J.*, **193**, 406.
———. 1980, *Ap. J.*, **238**, 585.
Eiroa, C., Hefile, H., and Qian, Z. Y. 1983, *Astr. Ap. Suppl.*, **54**, 309.
Elias, J. H., Frogel, J. A., Matthews, K., and Neugebauer, G. 1982, *A.J.*, **87**, 1029.
Gehrz, R. D., and Woolf, N. J. 1971, *Ap. J.* (*Letters*), **165**, L285.
Gillett, F. C., Low, F. J., and Stein, W. A. 1967, *Ap. J.* (*Letters*), **149**, L97.
Grasdalen, G. L. 1979, *Ap. J.*, **229**, 587.
Hanner, M. S., Tokunaga, A. T., Veeder, G. J., and A'Hearn, M. F. 1984, *A.J.*, **89**, 162.
Krishna Swamy, K. S., and O'Dell, C. R. 1968, *Ap. J.* (*Letters*), **151**, L61.
Kwok, S. 1980, *Ap. J.*, **236**, 592.
———. 1982, *Ap. J.*, **258**, 280.
———. 1985, *A.J.*, **90**, 49.
Kwok, S., and Bignell, R. C. 1984, *Ap. J.*, **276**, 544.
Kwok, S., Purton, C. R., and Keenan, D. W. 1981, *Ap. J.*, **250**, 232.
Kwok, S., Purton, C. R., Matthews, H. E., and Spoelstra, T. A. T. 1985, *Astr. Ap.*, **114**, 321.
Merrill, K. M. 1977, in *IAU Colloquium 42, The Interaction of Variable Stars with Their Environment*, ed. R. Kippenhahn, J. Rake, and W. Strohmeier, *Verôff. Remeis-Sterw. Bamberg*, Vol. **11**, No. 121, p. 446.
Maillard, J. P., and Dyck, H. M. 1982, in *Proc. 2nd ESO Infrared Workshop* (Garching: ESO), p. 29.
Milne, D. K. 1976, *A.J.*, **81**, 753.
———. 1979, *Astr. Ap. Suppl.*, **36**, 227.
Neugebauer, G., *et al.* 1984, *Ap. J.* (*Letters*), **278**, L1.
Pottasch, S. R. 1984, *Planetary Nebulae* (Dordrecht: Reidel).
Pottasch, S. R., *et al.* 1984, *Astr. Ap.*, **138**, 10.
Sinton, W. M., and Tittemore, W. C. 1984, *A.J.*, **89**, 1366.
Tokunaga, A. J. 1984, *A.J.*, **89**, 172.

B. J. HRIVNAK: Department of Physics, Valparaiso University, Valparaiso, IN 46393

S. KWOK and E. F. MILONE: Department of Physics, The University of Calgary, Calgary, Alberta, Canada T2N 1N4